

UNIVERSIDADE  
DE SANTIAGO DE COMPOSTELA

Facultade de Química

Study of the use of laser ablation  
coupled with SP-ICP-MS for the  
analysis of microplastics



Curso 2024/25

Alumno/a: María Pérez Costas

**Elena María Peña Vázquez**, tutora y docente del Departamento de Química Analítica, Nutrición y Bromatología de la Universidad de Santiago de Compostela, y **María del Carmen Barciela Alonso**, cotutora y docente del Departamento de Química Analítica, Nutrición y Bromatología de la Universidad de Santiago de Compostela, autorizan la presentación del Trabajo de Fin de Grado “Study of the use of laser ablation coupled with SP-ICP-MS for the analysis of microplastics” de la alumna María Pérez Costas en la convocatoria de julio del curso 2024/2025, el cual fue realizado bajo su dirección en los laboratorios del Grupo de Elementos Traza, Espectroscopía y Especiación (GETEE) perteneciente al Instituto de Materiales (iMATUS).

Y para que así conste firmamos el presente informe en Santiago de Compostela el 27 de junio del 2025.

Firmado por PEÑA VAZQUEZ ELENA MARIA -  
\*\*\*2939\*\* el día 27/06/2025 con un  
certificado emitido por AC FNMT Usuarios

BARCIELA ALONSO  
MARIA CARMEN -  
36077893R  
Firmado digitalmente por  
BARCIELA ALONSO MARIA  
CARMEN - 36077893R  
Fecha: 2025.06.27 14:16:27  
+02'00'

## **I. Glossary**

**CRM:** Certified reference material

**ICP-MS:** Inductively coupled plasma mass spectrometry

**IR:** Infrared spectroscopy

**LA:** Laser ablation

**LA-SP-ICP-MS:** Laser ablation single particle inductively coupled plasma mass spectrometry

**LOD:** Limit of detection

**MPs:** Microplastics

**NPs:** Nanoplastics

**PE:** Polyethylene

**PEEK:** Polyether ether ketone

**PMMA:** Polymethyl methacrylate

**PS:** Polystyrene

**PVC:** Polyvinyl chloride

**SP-ICP-MS:** Single particle inductively coupled plasma mass spectrometry

**μ-FTIR:** Fourier transformed infrared micro-spectroscopy

**μ-Raman:** Raman micro-spectroscopy

# Index

<b>1. ABSTRACT</b> .....	6
<b>1.1. Abstract</b> .....	6
<b>1.2. Resúmen</b> .....	6
<b>1.3. Resúmo</b> .....	7
<b>2. INTRODUCTION</b> .....	9
<b>2.1. Plastics and microplastics' history</b> .....	9
<b>2.2. Classification of microplastics</b> .....	10
<b>2.3. Microplastics in nature</b> .....	10
<b>2.4. The issue with microplastics</b> .....	11
2.4.1. <i>Solutions against these issues</i> .....	12
<b>2.5. The use of LA-SP-ICP-MS</b> .....	12
2.5.1. <i>Single particle ICP-MS</i> .....	12
2.5.2. <i>Laser ablation coupled with SP-ICP-MS</i> .....	14
<b>3. OBJECTIVES AND WORK PLAN</b> .....	16
<b>4. EXPERIMENTAL PROCEDURES</b> .....	17
<b>4.1. Instrumentation, materials and reagents</b> .....	17
4.1.1. <i>Instrumentation</i> .....	17
4.1.2. <i>Materials</i> .....	17
4.1.3. <i>Reagents</i> .....	17
<b>4.2. Preparation of standards for LA-SP-ICP-MS</b> .....	18
<b>4.3. Procedure of MPs characterization by Raman micro-spectroscopy</b> .....	19
<b>4.4. Procedure of MPs analysis by LA-SP-ICP-MS</b> .....	19
<b>5. RESULTS AND DISCUSSION</b> .....	22
<b>5.1. Characterization of MP standards by Raman micro-spectroscopy</b> .....	22
5.1.1. <i>Characterization of polyethylene MPs by Raman micro-spectroscopy</i> .....	22
5.1.2. <i>Characterization of the latex spheres by Raman micro-spectroscopy</i> .....	23
5.1.3. <i>Measuring the diameter of the latex spheres (2-9 <math>\mu\text{m}</math>) and PE microplastics (43-50 <math>\mu\text{m}</math>)</i> 25	
5.1.3.1. <i>Latex spheres (2-9 <math>\mu\text{m}</math>)</i> .....	25
5.1.3.2. <i>Polyethylene microplastics (43-50 <math>\mu\text{m}</math>)</i> .....	26
<b>5.2. Study of parameters affecting MPs analysis by LA-SP-ICP-MS</b> .....	26
5.2.1. <i>Optimization of the laser energy (spot size: 50 <math>\mu\text{m}</math>)</i> .....	27
5.2.2. <i>Optimization of the laser energy (spot size: 100 <math>\mu\text{m}</math>)</i> .....	28
5.2.3. <i>Influence of repetition rate and scan speed</i> .....	30

5.2.4.	<i>Influence of dwell time</i> .....	30
5.2.5.	<i>Influence of the carrier gas flow rate on the background signal</i> .....	32
<b>5.3.</b>	<b>Analytical characteristics of MP analysis by LA-SP-ICP-MS</b> .....	<b>33</b>
5.3.1.	<i>Calibration</i> .....	33
5.3.2.	<i>Reproducibility in the measurements</i> .....	34
5.3.3.	<i>Limit of detection in size of MPs by LA-SP-ICP-MS</i> .....	37
<b>6.</b>	<b>CONCLUSIONS</b> .....	<b>39</b>
6.1.	<b>Conclusions</b> .....	39
6.2.	<b>Conclusiones</b> .....	39
6.3.	<b>Conclusiones</b> .....	40
<b>7.</b>	<b>REFERENCES</b> .....	<b>41</b>

# **1. ABSTRACT**

## **1.1. Abstract**

Plastics and microplastics are one of the most important emergent contaminants in our society. They are present in aquatic ecosystems and are ingested by marine organisms, consequently, entering into the human food chain. These microplastics are known to be very harmful for human health and the environment, hence it is crucial to have fast methods of screening to understand their origin, impact and interaction with our surroundings. The study of the analysis of MPs using LA-SP-ICP-MS is essential to quickly provide information on the size and number of microplastics in a sample. This technique does not need a nebulizer which allows the elimination of MP size limitations. Moreover, MPs can be analysed directly on solid substrates e.g. collected in a filter, without other pretreatment.

In this project, several instrumental parameters were evaluated to improve the analysis of microplastics using LA-SP-ICP-MS. For the LA system, spot size and laser energy showed a great influence on the ablation efficiency, meanwhile scan speed and repetition rate did not show impact. For the SP-ICP-MS system, dwell time and carrier gas flow rate were crucial for minimizing the background signal, important for the detection of smaller MPs. Polyethylene powder and latex polystyrene spheres of certified sizes were used in the experiments. No significant difference was observed when evaluating suspensions in water or methanol. Moreover, fiberglass filters as substrate showed an improvement in retention of MPs compared to microscope slides. Finally, the precision and the limit of detection of the method were also determined.

## **1.2. Resumen**

Los plásticos y microplásticos son unos de los contaminantes emergentes más importantes en nuestra sociedad. Están presentes en los ecosistemas acuáticos y son ingeridos por organismos marinos, entrando así en la cadena alimentaria humana. Estos microplásticos son perjudiciales para la salud y medio ambiente, por tanto, es crucial contar con métodos rápidos de cribado para comprender su origen, impacto e interacción con nuestro entorno. El estudio del análisis de microplásticos mediante LA-SP-ICP-MS es esencial para obtener información rápida sobre el tamaño y cantidad de microplásticos en una muestra. Esta técnica no requiere nebulizador, permitiendo eliminar las limitaciones de tamaño de microplásticos.

Además, pueden analizarse directamente en sustratos sólidos, por ejemplo filtros, sin ningún pretratamiento.

En este proyecto, se evaluaron varios parámetros instrumentales para mejorar el análisis de microplásticos mediante LA-SP-ICP-MS. En LA, el tamaño y la energía del láser mostraron una gran influencia en la eficiencia de la ablación, mientras que la velocidad de escaneo y la tasa de repetición no mostraron impacto. En SP-ICP-MS, el tiempo de permanencia y el caudal del gas portador fueron cruciales para minimizar la señal del fondo, importante para la detección de MPs pequeños. Se utilizaron polvo de polietileno y esferas de látex de poliestireno de tamaños certificados. No se observaron diferencias significativas al evaluar suspensiones en agua o metanol. La utilización de filtros de fibra de vidrio como sustrato mostró una mejora en la retención de MPs comparado con los portaobjetos. Finalmente, se determinaron la precisión y el límite de detección del método.

### **1.3. Resumo**

Os plásticos e os microplásticos están entre os contaminantes emerxentes máis importantes da nosa sociedade. Están presentes nos ecosistemas acuáticos e son inxeridos polos organismos mariños, entrando así na cadea alimentaria humana. Estes microplásticos son moi prexudiciais para a saúde e o medio ambiente, polo que é importante contar con métodos rápidos de cribado para comprender a súa orixe, impacto e interacción co noso contorno. O estudo da análise de microplásticos mediante LA-SP-ICP-MS é esencial para obter información rápida sobre o tamaño e a cantidade de microplásticos nunha mostra. Esta técnica non require un nebulizador, o que elimina as limitacións de tamaño dos microplásticos. Ademais, os microplásticos pódense analizar directamente en substratos sólidos, por exemplo, en filtros, sen ningún pretratamento.

Neste proxecto, avaliáronse varios parámetros instrumentais para mellorar a análise de microplásticos mediante LA-SP-ICP-MS. En LA, o tamaño e a enerxía do láser mostraron unha influencia significativa na eficiencia da ablación, mentres que a velocidade de escaneo e a taxa de repetición non mostraron ningún impacto. En SP-ICP-MS, o tempo de residencia e o caudal do gas portador foron cruciais para minimizar o sinal do fondo, que é importante para a detección de microplásticos máis pequenos. Empregáronse po de polietileno e esferas de látex de poliestireno de tamaños certificados. Non se observaron diferenzas significativas ao avaliar as suspensións en auga ou metanol. Os filtros de fibra de vidro como substrato mostraron unha

mellor retención de MPs comparado cos portaobxectos. Finalmente, determináronse a precisión e o límite de detección do método.

## 2. INTRODUCTION

Plastic has become one of the most widespread materials since its beginnings. At its core, plastic was designed to improve human living conditions, but today it has become a real danger to the environment and the safety of the planet.<sup>1</sup>

The increasing presence of microplastics in the environment is causing serious pollution worldwide. The Commission's Delegated Decision (EU) 2024/1441 defines microplastic as a "small and discrete object, solid, insoluble in water and partially or totally made of synthetic polymers or chemically modified natural polymers".<sup>2</sup> Microplastics are easily introduced into the environment and persist there for a long time. The degradation of plastic waste generates microplastic (MP) or nanoplastic (NP) particles. This division is based on the diameter of the plastic fragments, with MPs having a diameter of less than 5 mm and NPs having a diameter of 1 to 1000 nm.<sup>1</sup>

### 2.1. Plastics and microplastics' history

Since the beginning of history, humans have put the effort to develop materials offering benefits not found in natural products. The development of plastics started with the use of natural materials that had intrinsic plastic properties, such as lightweight, durable and mouldable. Slowly, the evolution of plastics involved the chemical modification of natural materials such as rubber, collagen and galalite.<sup>3</sup>

The first synthetic polymer was invented in 1869 by John Wesley Hyatt, who was inspired by a New York firm's offer of \$10,000 for anyone who could provide a substitute for ivory. By treating cellulose derived from cotton fiber with camphor, Hyatt discovered a plastic that could be moulded into a variety of shapes and was able to imitate natural substances.<sup>4</sup>

The 20<sup>th</sup> century saw a revolution in plastic production: the beginning of entirely synthetic polymers. Belgian chemist Leo Baekeland was the first scientist to produce the first fully synthetic plastic in 1907. This plastic, which he would call bakelite, combined two chemicals, formaldehyde and phenol.<sup>5</sup>

The main creations in the world of plastic happened between the two World Wars: cellophane in 1913, then polyvinyl chloride in 1927, polystyrene and nylon in 1938 (used during the war for parachutes, ropes, and more) and polyethylene in 1942.<sup>6</sup>

In the 1960s, plastic began to be used in substitution of other more expensive materials, such as wood or packaging glass. In the 1980s, the production escalated, making it one of the most relevant industries worldwide. The investigation in order to achieve better formulas was diversified, what produced plastics with various chemical and physical properties.<sup>7</sup> Nowadays, there are more than 430 million tonnes of plastic produced annually.<sup>8</sup>

## **2.2. Classification of microplastics**

Microplastics can be divided into two different categories according to the European Parliament website:<sup>9</sup>

- Primary microplastics:
  - Small particles thrown directly to the environment.
  - It is estimated that they represent between the 15 % and 31 % of the microplastics in the oceans.
  - 35 % of primary microplastics come from the washing of synthetic clothing.
  - Tire abrasion represents the 28 %.
  - Microplastics added intentionally to personal care products are the 2 %.
- Secondary microplastics:
  - They are originated from the degradation of bigger plastic objects, such as plastic bags, bottles or fishing nets.
  - They represent between the 69 % and 81 % of the microplastics found in the oceans.

## **2.3. Microplastics in nature**

Plastic production is increasing sharply.<sup>10</sup> Most natural polymers that were once employed in our daily lives have now been replaced by plastics due to their high longevity, inertness, and relative affordability.<sup>11</sup> However, two-thirds of plastics are short-lived products that soon become waste, filling the ocean and, often, working their way into the human food chain.<sup>8</sup> This has raised concerns about the effects of microplastics and nanoplastics on human health. These concerns are partly influenced by alarming findings of the presence of microplastics in various human tissues, including the brain and placenta.<sup>10</sup> Continuing research is examining pathways of human exposure to microplastics. Most attention is focused on soil and water as common sources of plastics that enter the food chain.

The most recent studies estimate that between 5.95 and 15.11 million tons of plastic enter the oceans each year, either directly or through rivers. This enormous volume of trash is then carried by currents practically all over the globe. It is estimated that there are currently up to 236,000 tons of plastic particles floating on the surface of the world's various seas. This figure is based on the volume of particles collected by trawl nets. However, samples reveal that each liter of ocean surface water contains an average of 11.8 microparticles of plastic fibers.<sup>12</sup>

Moreover, microplastics were also detected in the atmosphere. Ambient air featured between <1 to >1000 microplastics/m<sup>3</sup> (outdoor) and <1 to 1583 ± 1181 microplastics/m<sup>3</sup> (indoor).<sup>13</sup> No difference was observed between indoor and outdoor concentrations of the minimum size of microplastics. Maximum microplastics sizes were larger indoors. In indoor areas, MPs behaviour is governed by room distribution, ventilation, and airflows. The main source of MPs in indoor air is considered to be synthetic textiles given that small fibres easily tear from clothes and other fibre products during wearing, cleaning and drying. The distribution and behaviour of MPs suspended in the atmosphere is like those of other airborne pollutants. Higher levels of MPs were observed in urban sites than those found in rural areas. This difference is attributed to intensified anthropogenic activities and higher population density in the urban site.<sup>14</sup>

#### **2.4. The issue with microplastics**

Microplastics are easily ingested due to their micro-level sizes. They also move easily through the food chain and persist in the environment since they are refractory to biodegradation. In addition, as microplastics exist in micro-level to nano-level sizes, they are virtually impossible to remove once released into the environment. Due to these characteristics, microplastics pose potential hazards to humans and the environment. In addition, microplastics can enter the human body when they are not filtered out during wastewater treatment processes, or they can reach the sea, posing risks for the ecosystems and humans.<sup>15</sup>

Microplastics are present in many environments and come from various sources. Many marine and aquatic organisms, including fish, birds, marine mammals, and invertebrates, mistake microplastics for food. This can lead to physical blockages, reduced feeding efficiency and causing malnutrition. Microplastics can also enter the food chain, starting from primary producers such as phytoplankton and algae and then progressing through various trophic levels.<sup>10</sup> Ingestion of microplastics is greatest in fishing communities and in populations

heavily dependent on a seafood diet. Consumption of contaminated fish and shellfish is a significant route of human exposure to marine microplastics and their chemical contaminants.<sup>16</sup>

Microplastics not only present inherent toxicity but they are also carriers for many pollutants to enter biological tissues and organs.<sup>17</sup> Toxicity may be caused by the polymer itself, unreacted monomers, impurities, additives, or other substances in the polymer matrix.<sup>15</sup> Although the health effects of microplastics are currently under investigation, studies indicate that exposure to these small plastic particles can potentially lead to various adverse effects on human health. Endocrine disruption is acknowledged as one of the potential effects of microplastics. Microplastics can contain and absorb various chemicals from the surroundings, including endocrine-disrupting compounds (EDCs). Also, inhalation of airborne microplastics can potentially affect the respiratory system by causing irritation and inflammation in the respiratory tract.<sup>18</sup>

#### *2.4.1. Solutions against these issues*

European deputies approved a strategy aimed at improving plastic management in the EU, which proposes that all plastic packaging be recyclable by 2030. They also called on the Commission to introduce a Europe-wide ban to eliminate the intentional addition of microplastics to cosmetic products and detergents by 2020. Parliament also demanded measures to minimize the release of microplastics from textiles, tires, paints, and cigarette butts. Parliament backed an EU ban on certain single-use plastic products, which make up 70 % of marine litter and for which non-plastic substitutes are available. Moreover, in 2015, Parliament voted in favor of a restriction in lightweight plastic bags in the European Union.<sup>9</sup>

## **2.5. The use of LA-SP-ICP-MS**

Inductively coupled plasma mass spectrometry (ICP-MS) is an analytical technique that can be used to measure elements at trace levels. ICP-MS has some important advantages, such as large analytical range, low sample volume, simple sample preparation, and the fact that is a multi-elemental technique with low detection limits.<sup>19</sup>

#### *2.5.1. Single particle ICP-MS*

Single particle inductively coupled plasma (SP-ICP-MS) takes advantage of the well-established elemental technique of ICP-MS but performing measurements on a “particle by particle” basis. More recently, the rapid increase in the development of engineered

nanomaterials has led to the interest on SP-ICP-MS as an alternative to other available techniques for detection, determination, and characterization of nanomaterials.<sup>20</sup>

The principle of SP-ICP-MS is that MPs are able to be detected individually if they are introduced sequentially into diluted suspensions and the detector is sufficiently fast to register them. The MPs generate discrete pulses of ions at a corresponding mass-to-charge ratio ( $m/z$ ) on the order of a few hundred of microseconds above the background signal. The intensity of the pulse is proportional to the mass of the MP. Moreover, the higher the signal the bigger is the particle. Also, the frequency of the detected signal pulses can be related to the particle number concentration in the suspension.<sup>21</sup> A time-resolved intensity profile is shown in Figure 1; where MPs of increasing sizes were analysed. It is possible to observe the proportional relationship between the MP size and the  $^{13}\text{C}$  signal intensity.

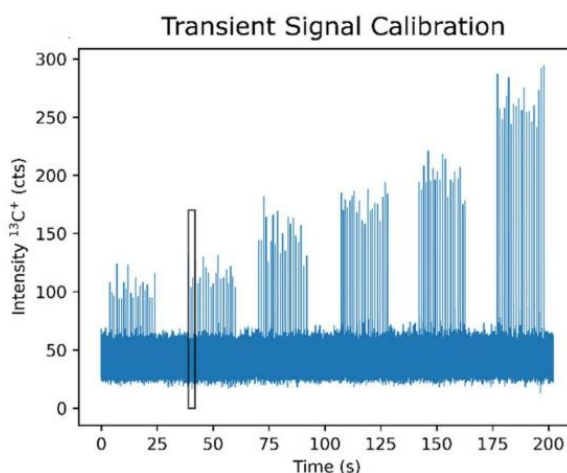


Figure 1. A time-resolved intensity profile for the measurement of increasing MP sizes.<sup>22</sup>

In terms of elements, carbon is very rarely determined by ICP-MS. The main reasons why carbon is not determined routinely by ICP-MS are the low sensitivity of the element and its high background levels.<sup>23</sup> However, the main element in microplastics and nanoplastics is carbon. As carbon is present everywhere, a high background signal is expected. In general, less abundant  $^{13}\text{C}$  isotope is monitored instead of the most abundant  $^{12}\text{C}$  isotope to prevent signal overloading.<sup>24</sup>

The Commission's Delegated Decision (EU) 2024/1441 stated that the microplastics in waters intended for human consumption should be collected by filtration through a cascade of four filters. The Delegated Decision also recommended two main analytical techniques: infrared (IR) and Raman optic micro-spectroscopy.<sup>2</sup> Fourier transformed infrared micro-spectroscopy ( $\mu$ -FTIR) is a variation of the infrared spectroscopy (IR) which combines a FTIR

spectrometer with a microscope to achieve spatially resolved IR spectra and the ability to obtain images; and the same happens for the Raman micro-spectroscopy ( $\mu$ -Raman). Moreover, the Delegated Decision recommends this methodology for microplastics from 15 mm to 20  $\mu$ m. However, SP-ICP-MS, compared to the techniques described previously, has relevant advantages. For the screening of microplastics, it is possible to count particles much faster, with lower size, detection limits, and if the particles are labelled with metals, it is possible to analyse nanoplastics.<sup>25</sup>

Even though conventional single-particle ICP-MS using MP liquid suspension as samples provides valuable analytical information for both natural and engineered nanoparticles, the measurement in suspension comes with challenges. Problems include the limited stability of particles in suspension over time, the low transport efficiency of standard pneumatic nebulizers as well as interferences from the suspension medium due to the presence of dissolved carbon in water, mainly atmospheric CO<sub>2</sub>.<sup>26</sup> However, there is the possibility of direct analysis by laser ablation (LA) which adds spatial-resolution characteristics for located microplastic analysis.<sup>27</sup>

#### *2.5.2. Laser ablation coupled with SP-ICP-MS*

Laser ablation is a process in which a laser beam is used as the main tool for the removal of a small portion of the target material. A laser, as a higher concentrated energy source, is centered at a specific place of the target material for the evaporation of light-absorbing materials. Surface atoms are removed by a multiphoton excitation process. Briefly, when the laser beam is centered on a target material in an ambient (liquid or gas) medium, it increases the temperature of the irradiated spot and evaporates it. The evaporated species and the surrounding molecules collide with each other, which results in the excitation of the electron state coupled with light emission and generation of ions and electrons, thus forming a laser-induced plasma plume.<sup>28</sup>

The benefits of using laser ablation include the direct analysis of nanoparticles in the solid sample and the intact particle transport, which also makes spatial information available. However, one drawback of laser ablation in bulk and imaging applications is the need for matrix-matched calibration standards that can be solid certified reference material or in-house prepared standards using various techniques, which tends to be tedious and complex. Nevertheless, a large number of trace elements in minerals have been determined accurately using non-matrix matched calibration and internal standardization.<sup>26</sup>

Laser ablation was recently characterized as a method for sampling and introducing microplastic particles into and inductively coupled plasma (ICP) for subsequent  $^{13}\text{C}$  monitoring using an ICP-MS operated in single-event mode. Using LA-SP-ICP-MS overcomes some drawbacks experienced using SP-ICP-MS. LA-SP-ICP-MS does not need nebulizer which allows not to have a limited size on the MPs. Also, MPs can be analysed directly when collected in a filter,<sup>29</sup> and the interference of the solvent is eliminated. Figure 2 shows a scheme of the introduction of one MP at a time in the SP-ICP-MS system with the corresponding time-resolved intensity profile, where the intensity of the signal is proportional to the mass of the MP, and the histogram, where the signal distribution of the MPs is represented.

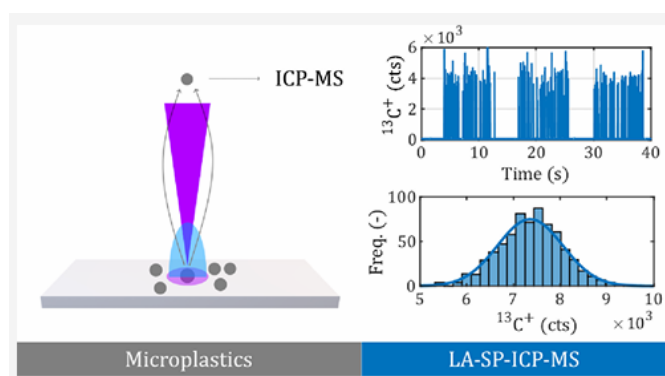


Figure 2. Scheme of introduction of one MP at a time and the corresponding time-resolved intensity profile and histogram.<sup>29</sup>

However, there are only two scientific papers that use this technique for the determination and quantification of MPs. Therefore, Van Acker *et al.* (2023)<sup>29</sup> uses LA-SP-ICP-MS to analyse three different types of MPs (PS, PMMA and PVC) and sizes from 2-20  $\mu\text{m}$ . In the experiments, they observed that single-shot analysis separated clustered MPs, allowing the analysis of individual particles. Moreover, the  $^{13}\text{C}$  signal intensity correlated linearly with the absolute C mass in the 2-10  $\mu\text{m}$  size range. The second study that uses this technique for the analysis of MPs was reported by Brunnbauer *et al.* (2025) where a new calibration approach that uses a PS thin film for the sizing of MPs is presented.<sup>22</sup> The calibration was performed by introducing defined amounts of carbon into the ICP-MS by ablating the PS thin film with different laser spot sizes. In addition, there are some scientific papers that use this technique for the analysis of metallic nanoparticles, such as the one written by Wang *et al.* (2022)<sup>30</sup> which is focused on studying the *in vivo* degradation of silver nanoparticles.

### **3. OBJECTIVES AND WORK PLAN**

Microplastics are easily introduced into the environment and persist there for a long time, making their way into sea life and human diets. Due to these problems, it is very important to develop fast screening techniques that can estimate the number and size of MPs present and select the samples that will be submitted to  $\mu$ -FTIR and  $\mu$ -Raman.

The main objective of this project is the study of the parameters that affect the analysis of microplastics using laser ablation coupled with SP-ICP-MS.

The parameters studied will be those related to laser ablation (laser energy, spot size, repetition rate and scan speed) and the measurements by SP-ICP-MS (dwell time, carrier gas flow rate). The effect of the deposition of MPs as water or methanol suspensions in different substrates (microscope slides or fiberglass filters) will be also evaluated. Finally, an estimation of the precision and the limit of detection of the measurements will be performed.

## 4. EXPERIMENTAL PROCEDURES

### 4.1. Instrumentation, materials and reagents

#### 4.1.1. Instrumentation

- NexION 2000 ICP-MS spectrometer, PerkinElmer, (Waltham, MA, USA) equipped with Nano-Syngistix™ Software for ICP-MS v.2.5, PerkinElmer, (Waltham, MA, USA)
- ESI NWR 213 laser ablation system (ESI New Wave Research Co., Cambridge, UK)
- Vortex mixer, Heidolph, (Schwabach, Germany)
- Centrifuge 2K15, Sigma Laborzentrifugen GmbH, (Osterode am Harz, Germany) equipped with a 12148H rotor
- WITec Confocal RAMAN Microscope. Model ALPHA 300R+, Oxford Instruments, (Abingdon, Oxfordshire, England) equipped with WITec Project FIVE software

#### 4.1.2. Materials

- Various glassware (microscope slides, vials, etc.)
- Eppendorf tubes
- Micropipettes of variable volumes with tips
- Glass microfiber filters, 37 mm, 1  $\mu\text{m}$  pore size, FVC037, Albet, (Dassel, Germany)

#### 4.1.3. Reagents

- Polyethylene powder (ultra high molecular weight, 43-50  $\mu\text{m}$  particle size), Sigma-Aldrich, (Osterode, Germany)
- Certified Reference Materials (CRMs), BCR, (Geel, Belgium):
  - Latex spheres BCR®-167 of 9.4  $\mu\text{m}$  in aqueous suspension ( $9,475 \pm 0.018 \mu\text{m}$ ). Concentration: 14 g/L
  - Latex spheres BCR®-166 of 4.8  $\mu\text{m}$  in aqueous suspension ( $4.821 \pm 0.019 \mu\text{m}$ ). Concentration: 2 g/L
  - Latex spheres BCR®-165 of 2.2  $\mu\text{m}$  in aqueous suspension ( $2.223 \pm 0.013 \mu\text{m}$ ). Concentration: 0.2 g/L
- Ultrapure water (18.2 M $\Omega$  cm of resistivity) obtained from a Milli-Q® IQ 7003 purification device system, (Millipore, Bedford, MA, USA).

- Certified Reference Material, Trace elements in glass NIST<sup>®</sup> SMR<sup>®</sup> 612 (Washington, USA)
- Helium (99.999%), Nippon Gases, (Madrid, Spain).

#### 4.2. Preparation of standards for LA-SP-ICP-MS

Previously to the deposition of the drops in the microscope slide, latex spheres standards must undergo a specific preparation. The aliquots taken from the vial shall be washed with ultrapure water in order to remove the surfactant that is used as stabilizer. The following procedure was employed:

1. First, place 200  $\mu\text{L}$  of latex particle suspension in an Eppendorf tube.
2. Afterwards, centrifuge in order to collect the solids in the bottom of the Eppendorf tube. The centrifugation process was performed for 15 minutes at 10000 rpm which translates into a g-force of 9168.
3. Carefully, withdraw the supernatant from the solids.
4. Resuspend the particles with 200  $\mu\text{L}$  of ultrapure water.
5. This process should be repeated three times.

As for the preparation of the standards, a suspension of 10 mg MP/mL is first prepared. Afterwards, this suspension is diluted to obtain a concentration range from 8 mg/mL to 1 mg/mL. Furthermore, two 10  $\mu\text{L}$  drops of each concentration are placed in a microscope slide close to the frosted end, drawing on the other side of the microscope slide four dots that form a square defining the edges of the drops as shown Figure 3. When performing the dilution is important to check that the solute is well suspended; if it is not, the vortex mixer should be used.

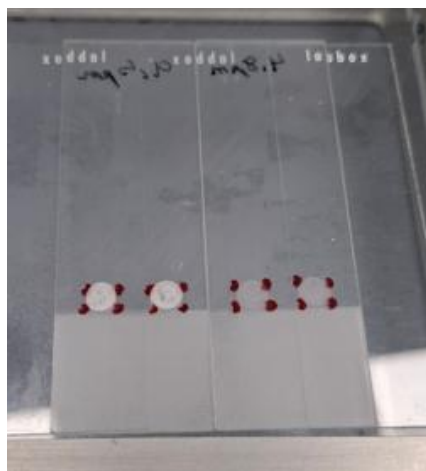


Figure 3. Placement of the samples in the microscope slides.

### 4.3. Procedure of MPs characterization by Raman micro-spectroscopy

The Raman micro-spectroscopy characterization is performed with the WITec Confocal RAMAN Microscope equipped with a laser of 532 nm. The MPs are held in a microscope slide and the spectra is registered and compared with the library. Moreover, pictures of the MPs are taken. The data obtained was treated with the WITec Project FIVE software.

### 4.4. Procedure of MPs analysis by LA-SP-ICP-MS

For the analysis of microplastics using LA-SP-ICP-MS, many parameters affecting the measurements must be taken into account.

Firstly, the positioning of the samples in the laser ablating chamber is crucial. The microscope slide with the sample must be even with the edges of the sample cell in order to achieve a good measurement, otherwise it will be very difficult to focus the samples.

The laser must strike the sample at the same distance in all the area. Therefore, the plate, where the microscope slide is held, must be flat. To achieve this, a bubble level is used as shown in Figure 4.

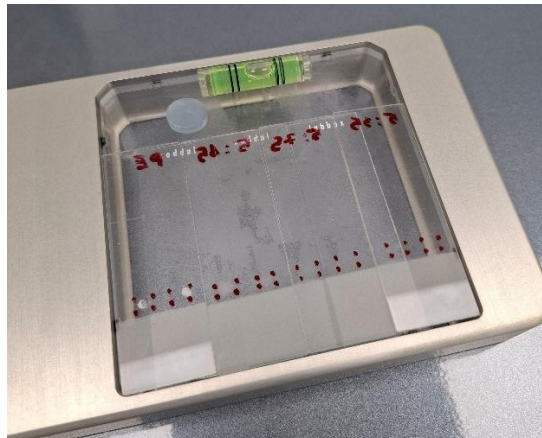


Figure 4. Bubble level to achieve an even plate.

Before the experiments, the system must be tuned using the CRM Trace elements in glass NIST<sup>®</sup> SMR<sup>®</sup> 612 to select the Ar nebulization flow, the position of the torch and the quadrupole voltages. The signal intensities are maximized without increasing the amount of oxides in the plasma ( $^{232}\text{Th}^{16}\text{O}/^{232}\text{Th} < 0.02$ ) or changing the elemental ratios present in the sample ( $^{232}\text{Th}/^{238}\text{U} > 0.07$ ). Table 1 shows the laser ablation conditions selected for this procedure.

Table 1. Operational conditions for NIST<sup>®</sup> SMR<sup>®</sup> 612 measurements by LA-SP-ICP-MS.

LA parameters (units)	Value
Laser	Nd:YAG (213 mm)
Scan speed (µm/s)	10
Laser energy (%)	20
Spot size (µm)	50
Repetition rate (Hz)	20
He pressure (psi)	0.3
He flow rate (mL/min)	300
Ablation pattern	5-mm-long straight line
Ablation time (min)	8
Isotopes monitored	<sup>7</sup> Li, <sup>24</sup> Mg, <sup>115</sup> In, <sup>140</sup> Ce, <sup>208</sup> Pb, <sup>232</sup> Th, <sup>238</sup> U

Table 2 shows the typical conditions selected for the analysis of MPs during the ablation of the 2-mm-long straight line in the samples. The abundance of <sup>13</sup>C was measured for monitoring microplastics and the Nano-Syngistix<sup>™</sup> Software was used to register the number of MPs and to calculate their diameter.

Table 2. Operational conditions for MPs analysis by LA-SP-ICP-MS.

LA parameters (units)	Value
Laser	Nd:YAG (213 nm)
Scan speed ( $\mu\text{m/s}$ )	20
Fluence ( $\text{J/cm}^2$ )	0.5 - 3.0
Spot size ( $\mu\text{m}$ )	100
Repetition rate (Hz)	20
He pressure (psi)	0.3
He flow rate (mL/min)	300
Ablation pattern	2-mm-long straight line
Ablation time	1 min 30 s
Ablation depth ( $\mu\text{m}$ )	0
Laser warm-up (s)	10
Laser wash-out (s)	15
SP-ICP-MS parameters (units)	Value
Tygon <sup>®</sup> interface tube	3.5 m length
Cone material	Nickel
Radiofrequency power (W)	1600
Plasma gas flow (L/min)	15
Auxiliary gas flow (L/min)	1.2
Nebulizer gas flow (L/min)	1.0 - 1.1 (daily optimized)
Dwell time ( $\mu\text{s}$ )	100
Acquisition time (s)	95
Readings	$9.5 \times 10^5$
Operation mode	Standard
Isotope	$^{13}\text{C}$
Voltage applied (V)	-17.5 (daily optimized)
Rejection parameter q (RPq)	0.25
MP density ( $\text{g/cm}^3$ )	0.95
MP mass fraction (%C)	92.31

## 5. RESULTS AND DISCUSSION

### 5.1. Characterization of MP standards by Raman micro-spectroscopy

#### 5.1.1. Characterization of polyethylene MPs by Raman micro-spectroscopy

The characterization of the polyethylene powder was carried out with Raman micro-spectroscopy using the WITec Confocal RAMAN Microscope; the spectrum obtained is shown in Figure 5. Polyethylene is a thermoplastic polymer, which means that gets soften with heat. Its repetition unit is  $(\text{CH}_2\text{-CH}_2)_n$  and its monomer is ethylene  $\text{CH}_2=\text{CH}_2$ .

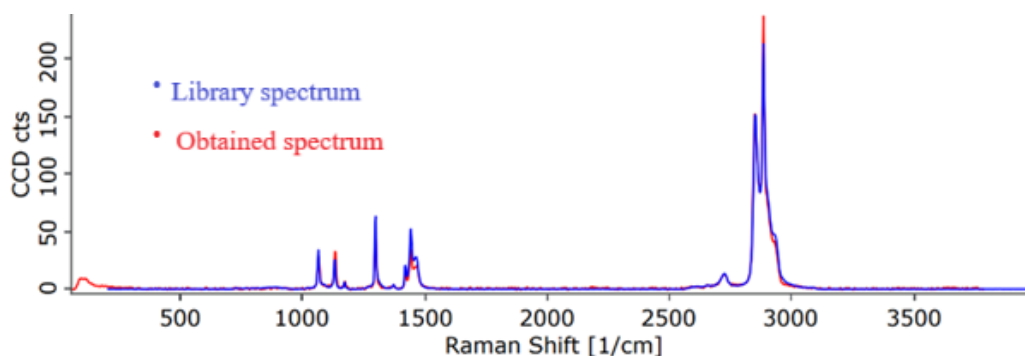


Figure 5. Raman spectrum of polyethylene MPs.

It is observed, mainly, the presence of two groups of peaks. The first one between 1000 and 1500  $\text{cm}^{-1}$  and the other one between 2800 and 3000  $\text{cm}^{-1}$ . The first group of peaks represent the stretching of the C-C bonds and the group of peaks around 2900  $\text{cm}^{-1}$  represents the stretching of the C-H bonds. Moreover, in Figure 6, an image of the PE particles is shown.

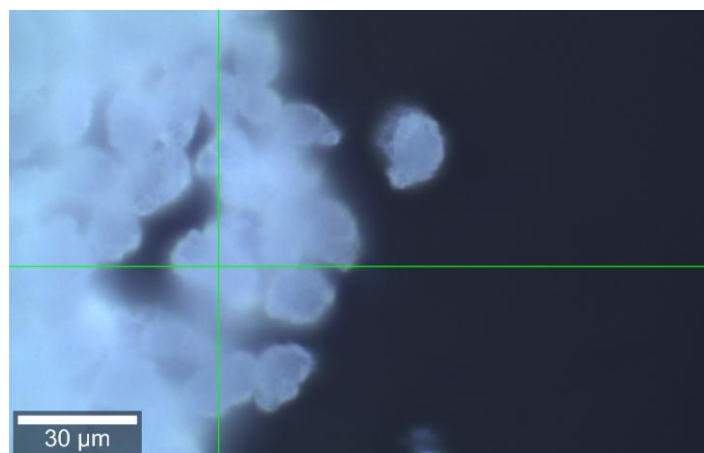


Figure 6. Image of the polyethylene sample.

### 5.1.2. Characterization of the latex spheres by Raman micro-spectroscopy

There are 3 sizes of the Certified Reference Materials available that are called “latex spheres”. The mean certified sizes are 2.223, 4.821 and 9.475  $\mu\text{m}$ . Each size of latex spheres was analysed by Raman micro-spectroscopy using WITec Confocal RAMAN Microscope. The latex spheres were analysed, getting the spectrum showed in Figure 7.

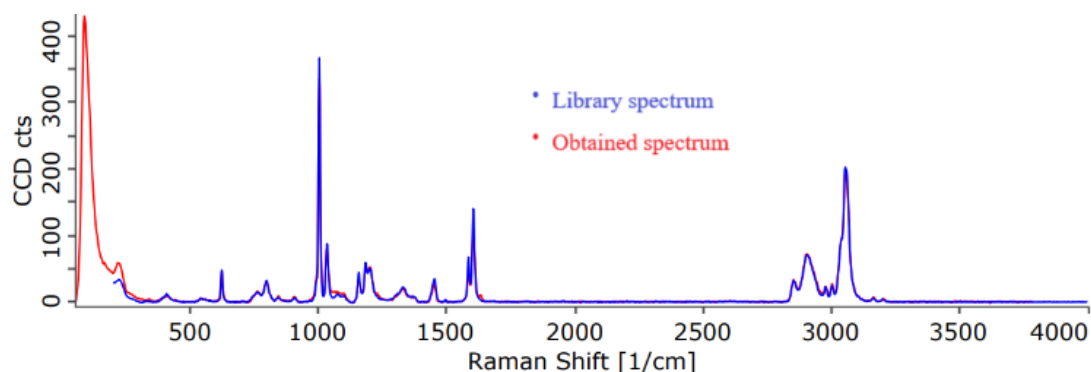
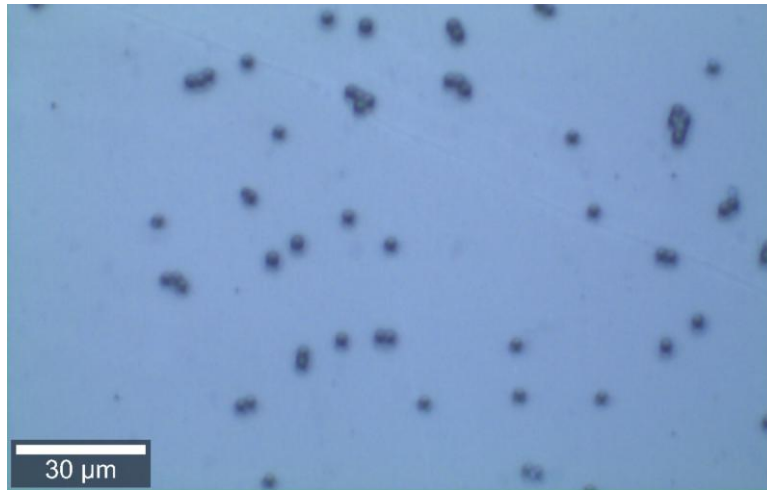


Figure 7. Raman spectrum of the Latex spheres.

The match achieved was with polystyrene. PS is a thermoplastic polymer. Its repetition unit is  $(\text{CHPh-CH}_2)_n$  and its monomer is styrene  $\text{CHPh=CH}_2$ . The assignation of the peaks starts with the peak around  $1000\text{ cm}^{-1}$  which represents the vibration of the aromatic ring. The peaks around  $1155\text{ cm}^{-1}$  represent the vibration of the C-H bond from the ring. The peaks around  $1600\text{ cm}^{-1}$  correspond to the stretching of the C=C bond from the ring. Lastly, the peaks around  $3000\text{ cm}^{-1}$  correspond to the stretching of the C-H bond of the main chain.

Moreover, pictures of the Latex spheres were taken. As shown in Figures 8, 9, 10 and 11, it can be observed that the larger the microplastics the higher is their tendency to agglomerate. Figure 8 represents the 2.223  $\mu\text{m}$  latex spheres; there are a big amount of them that are not agglomerated, it is possible to find individual microplastic particles.



*Figure 8. Image of 2.223 μm latex spheres.*

Figure 9 represents the 4.821 μm latex spheres, it can be observed that, since they are bigger microplastics, some of them start to agglomerate and it starts to get difficult to find individual microplastic particles.

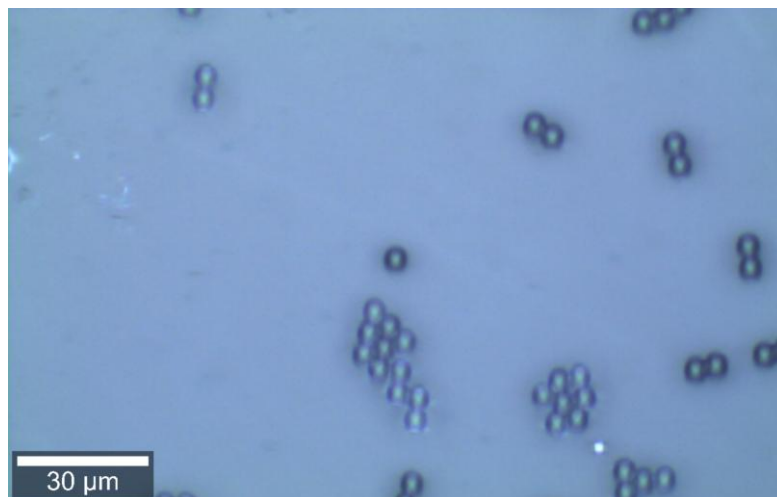


*Figure 9. Image of 4.821 μm latex spheres.*

Finally, Figure 10 and Figure 11 show the 9.475 μm latex spheres. As it is shown, it was very difficult to find one single microplastic that was not agglomerated. Figure 11 shows that all microplastics are agglomerated forming a net-like structure, there are no single microplastic particles in the sample.

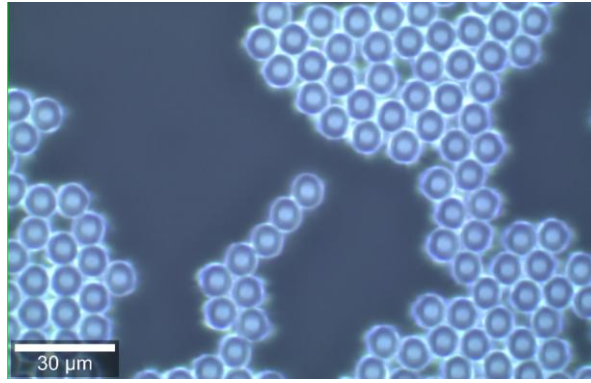


Figure 10. Image of 9.475 μm latex spheres.

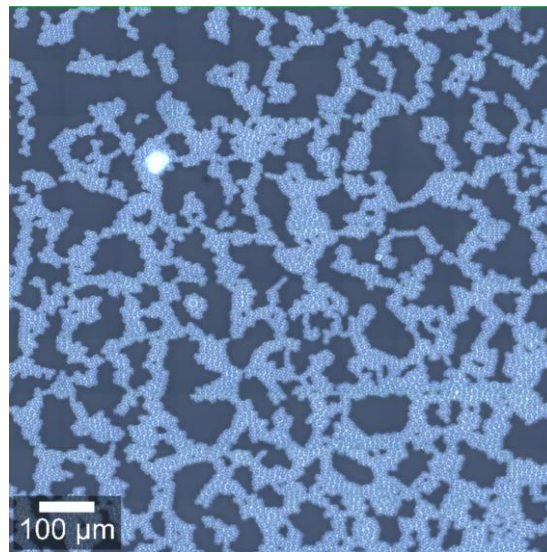


Figure 11. Larger image of 9.475 μm latex spheres.

### 5.1.3. Measuring the diameter of the latex spheres (2-9 μm) and PE microplastics (43-50 μm)

In order to measure the diameter of the samples of latex spheres and polyethylene powder, the WITec Project FIVE software was used to visualize the images taken of the samples. Using the cursor and clicking from one edge to the opposite one of a particle, 50 particles of each sample were measured.

#### 5.1.3.1. Latex spheres (2-9 μm)

The diameters of the latex spheres, with their 95 % confidence intervals, provided by the Certified Reference Materials (CRMs) are  $9.475 \pm 0.018 \mu\text{m}$  ( $n = 5$ ),  $4.821 \pm 0.019 \mu\text{m}$  ( $n = 5$ ) and  $2.223 \pm 0.013 \mu\text{m}$  ( $n = 4$ ). However, after measuring them with the help of the images taken with the WITec Confocal RAMAN Microscope, the following diameters were obtained:  $9.517 \pm 0.085 \mu\text{m}$ ,  $4.831 \pm 0.145 \mu\text{m}$  and  $2.574 \pm 0.158 \mu\text{m}$  (mean  $\pm$  standard deviation,  $n = 50$ ).

A t-test, to compare independent means, was performed in order to check if there was a significant statistical difference between the certified sizes and the experimental measurements. An F-test was previously conducted to compare the standard deviations that were found to be statistically different ( $P < 0.05$ ). The results showed that there was a statistical difference for 9.475 and 2.223  $\mu\text{m}$  latex spheres ( $P < 0.05$ ), probably due to the limited resolution of the Raman micro-spectroscopy images. Moreover, the 2.223  $\mu\text{m}$  MPs are close to the size detection limit of  $\mu$ -Raman; hence these results were expected.

#### 5.1.3.2. *Polyethylene microplastics (43-50 $\mu\text{m}$ )*

The PE powder used for this project is from Sigma-Aldrich. According to the manufacturer, the particle size is between 43 and 50  $\mu\text{m}$ . It was confirmed manually; measurements generated an average size of  $46.442 \pm 2.895 \mu\text{m}$  (mean  $\pm$  standard deviation,  $n = 50$ ).

## 5.2. Study of parameters affecting MPs analysis by LA-SP-ICP-MS

The first studies that were performed with laser ablation were done with the polyethylene powder. The theoretical particle size was between 34-50  $\mu\text{m}$ . This MP with a big size was chosen to get a higher sensitivity when measuring  $^{13}\text{C}$  abundance.

After the ablation of the NIST<sup>®</sup> SRM<sup>®</sup> 612 standard to tune the instrument, a microscope slide was introduced in the laser ablation chamber with a 10  $\mu\text{L}$  drop of the 10 mg/mL polyethylene suspension. Firstly, once the drop of sample was found with the camera, the coordinates were set, the red spots that were drawn in the preparation of the standards helped to identify the edges. For this first drop, the coordinates obtained were:

1. Spot in the top left: (60.705, 46.304, 7.9)
2. Spot in the top right: (64.653, 46.304, 7.9)
3. Spot in the bottom right: (64.653, 49.353, 7.9)
4. Spot in the bottom left: (60.7, 49.353, 7.9)

In this way, a rectangular shape, where several measurements were going to take place, was formed. Once the coordinates were set, the optimization of the laser energy was carried out.

### 5.2.1. Optimization of the laser energy (spot size: 50 $\mu\text{m}$ )

The laser energy, defined as the energy delivered per unit of area measured in  $\text{J}/\text{cm}^2$ , is a key parameter in laser ablation. Its optimization is crucial because depending on the amount of energy applied, the efficiency of the ablation is compromised. If the laser energy is too small, many MPs are not going to be ablated, whereas excessive laser energy could lead to elemental fractionation and potential damage on the substrate employed.

Furthermore, the spot size can play an important role in fractionation effects and signal intensity for constant laser energies. The smaller spot sizes induce greater variation in signal intensity and elemental ratio. Larger spot sizes produce less fractionation achieving a better representation of the material.<sup>31</sup> The optimization of the laser energy was performed with two different spot sizes.

For a spot size of 50  $\mu\text{m}$ , the measurements were performed with the following conditions: Scan speed 20  $\mu\text{m}/\text{s}$ , repetition rate 20 Hz and energies from 1 to 5  $\text{J}/\text{cm}^2$ . The number of signals obtained with each laser energy is shown in Figure 12. As shown in the figure, the greatest number of peaks were achieved employing an energy of 3  $\text{J}/\text{cm}^2$ .

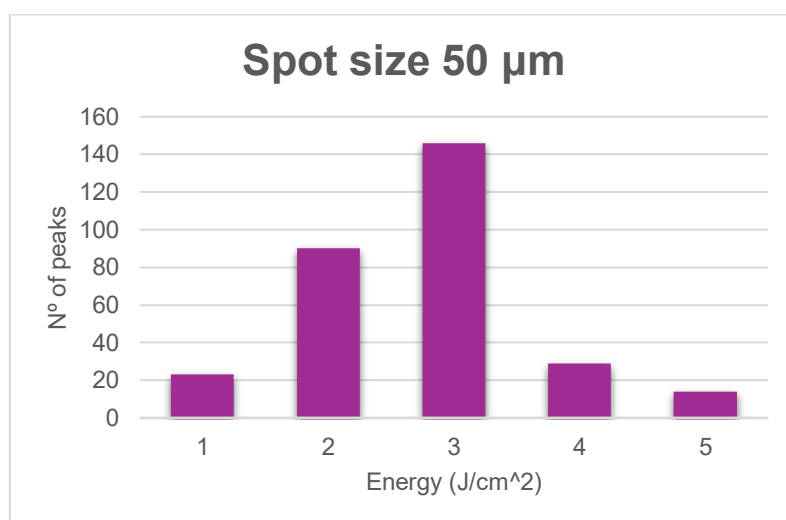


Figure 12. Influence of laser energy on the number of MP signals (spot size: 50  $\mu\text{m}$ ).

However, when ablating the microplastics with high laser energies, such as 4 and 5  $\text{J}/\text{cm}^2$ , a black line in the microscope slide was observed; it seems that these energies were too strong and they damaged the microscopic slide as shown in Figure 13 and Figure 14. Also, it was observed that the laser was pushing the MPs away instead of ablating them; this would explain the low number of signals obtained for these energies.

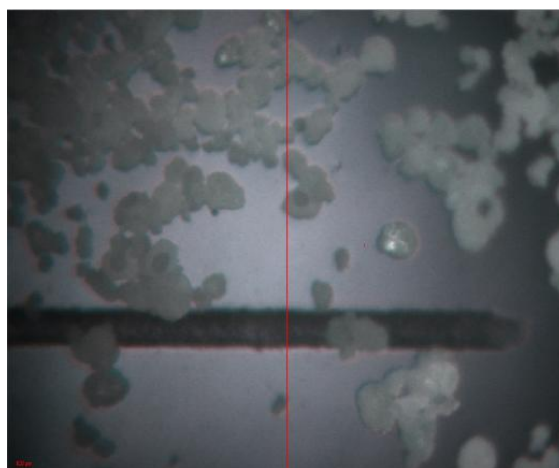


Figure 13. Damage of microscope slide using energy  $5 \text{ J/cm}^2$  (spot size =  $50 \mu\text{m}$ ).

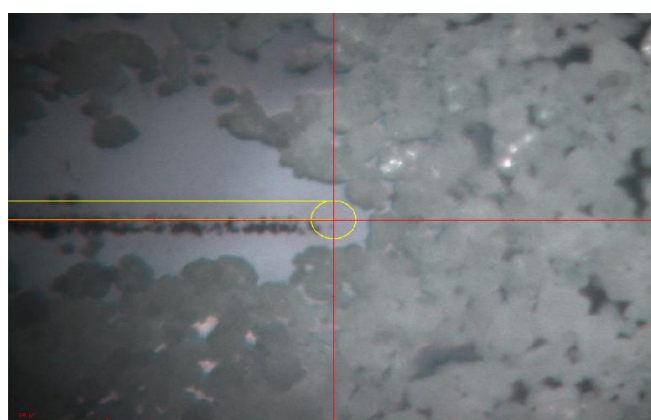


Figure 14. Damage of microscope slide using energy  $4 \text{ J/cm}^2$  (spot size =  $50 \mu\text{m}$ ).

Finally, after comparing all energies, it was observed that with these conditions, scan speed  $20 \mu\text{m/s}$ , repetition rate  $20 \text{ Hz}$ , spot size  $50 \mu\text{m}$ ; an energy of  $3 \text{ J/cm}^2$  was the most suitable, obtaining 146 peak signals.

#### 5.2.2. Optimization of the laser energy (spot size: $100 \mu\text{m}$ )

After optimizing the influence of the laser energy for spot size  $50 \mu\text{m}$ , a comparison of 2 different spot sizes was performed. The comparison was between  $50 \mu\text{m}$ , which was the one used first for the optimization of the laser energy, and  $100 \mu\text{m}$ . The first experiment was carried out with a laser energy of  $3 \text{ J/cm}^2$  since it is the one that gave more  $^{13}\text{C}$  peak signals in the previous optimization. The following conditions were used for the measurement: Scan speed  $20 \mu\text{m/s}$ , repetition rate  $20 \text{ Hz}$ , spot size  $100 \mu\text{m}$  and energy  $3 \text{ J/cm}^2$ . It was observed that 244 peaks were obtained, but with a lot of damage in the microscope slide as shown in Figure 15.

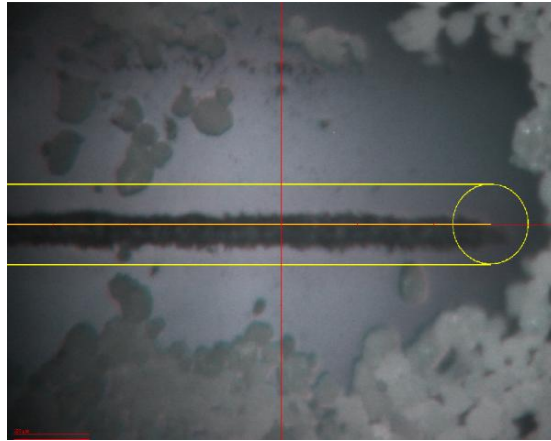


Figure 15. Damage in microscope slide with energy 3 J/cm<sup>2</sup> (spot size 100 μm).

Furthermore, it was decided to perform the measurement with energies 0.5, 1 and 2 J/cm<sup>2</sup>. As shown in Figure 16, the best results were obtained for a laser energy of 2 J/cm<sup>2</sup>.

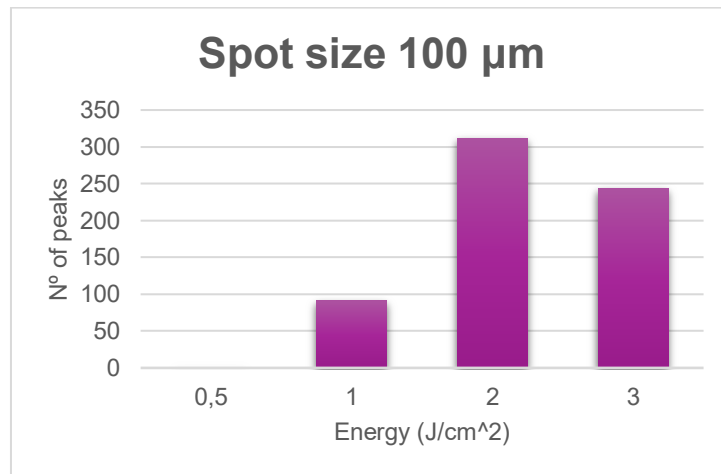


Figure 16. Influence of laser energy on the number of MP signals (spot size: 100 μm).

Energy 0.5 J/cm<sup>2</sup> was too weak giving 0 peak signals. As for energy 1 J/cm<sup>2</sup>, not all the microplastics were ablated leaving a lot of them behind and not measured, as shown Figure 17.

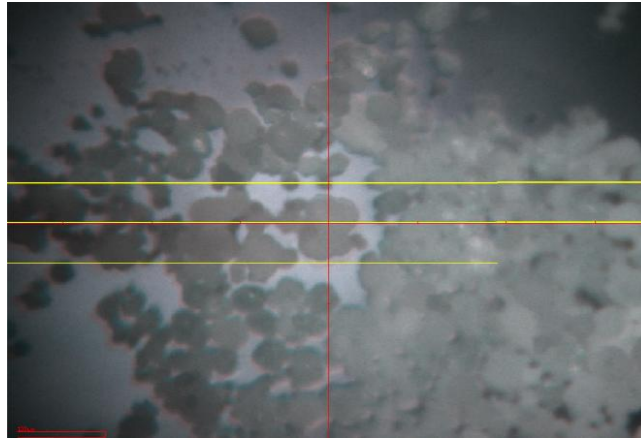


Figure 17. Microplastics after ablating with laser energy 1 J/cm<sup>2</sup>.

As a conclusion, taking into account the laser energy and the spot size, the higher amount of <sup>13</sup>C peak signals for MPs was obtained using the conditions of scan speed 20 μm/s, repetition rate 20 Hz, spot size 100 μm and laser energy 2 J/cm<sup>2</sup>.

#### 5.2.3. Influence of repetition rate and scan speed

The repetition rate is the amount of laser pulses emitted per second, usually measured in Hertz (Hz). As for the scan speed, it refers to the rate at which the laser beam moves through the material. After performing several measurements, changing the values of these parameters; significant changes were not observed.

#### 5.2.4. Influence of dwell time

- Relationship between dwell time and MP peak signal

The selection of the dwell time (duration of each measurement) and the broadness of the peak signal are very much related. If the dwell time is small, a decent measurement is not possible to obtain because the signal registered is too small. However, if the dwell time is too big, it is very difficult to observe a signal if there is a small number of MPs. In order to check if the dwell time used in the measurements is adequate, a measurement was carried out using the PE powder samples as standards to get the shape of the peak. In Figure 18, the peak profile obtained for this sample is shown.

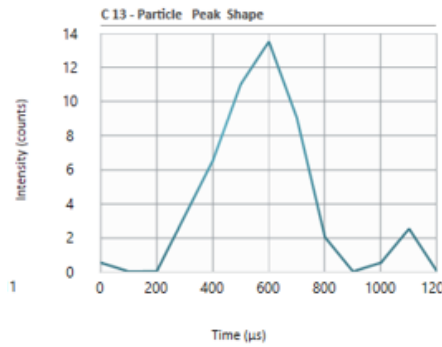


Figure 18. Peak shape of the polyethylene standard.

The peak obtained goes, approximately, from 200 to 800  $\mu\text{s}$ . Considering a dwell time of 100  $\mu\text{s}$ , a total of 6 measurements are being performed. This number of measurements is very common for SP-ICP-MS. Furthermore, many other research papers use this dwell time in their experiments.<sup>29</sup>

- Relationship between the dwell time and the background signal

The dwell time and the background signal recorded in the measurements are tightly correlated. It was observed that the background changes proportionally with the dwell time (Figure 19). As shown in the Figure 19, the bigger is the dwell time, the higher the background signal is going to be. Therefore, the dwell time of 100  $\mu\text{s}$  was used as a compromise decision.

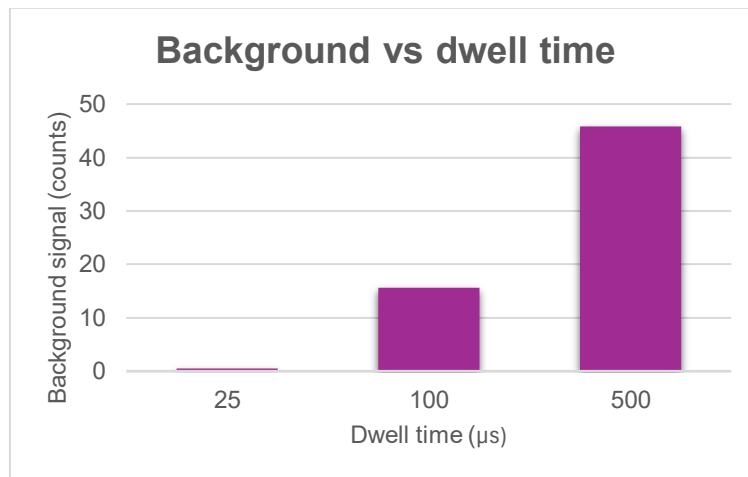


Figure 19. Influence of the dwell time on the background signal.

### 5.2.5. Influence of the carrier gas flow rate on the background signal

The carrier gas, usually helium (He) or argon (Ar), is critical for transporting the ablated particle sample from the laser ablation chamber to the ICP-MS. It is known that the carrier gas influences the particle deposition around the ablation crater. The use of He seems to reduce the particle deposition and increase the signal intensity.<sup>32</sup>

However, the selection of the carrier gas flow rate has to be done thoughtfully because it was observed that there was a proportional influence on the carrier gas flow rate and the background signal. As shown in Figure 20, there is a linear relationship between the He flow rate and the background signal. If the background is too high, the smaller MPs are not detected because their signals cannot be differentiated from the background signal. However, when the background signal is very small, the carrier gas flow rate is also very small, not being able to carry the ablated sample. Therefore, a carrier gas flow rate of 300 mL/min (0.3 psi) was used as a compromise decision.

In further investigations, changing the Tygon<sup>®</sup> tubes of the equipment for PEEK (polyether ether ketone) tubes should be also considered for lowering the background signal.

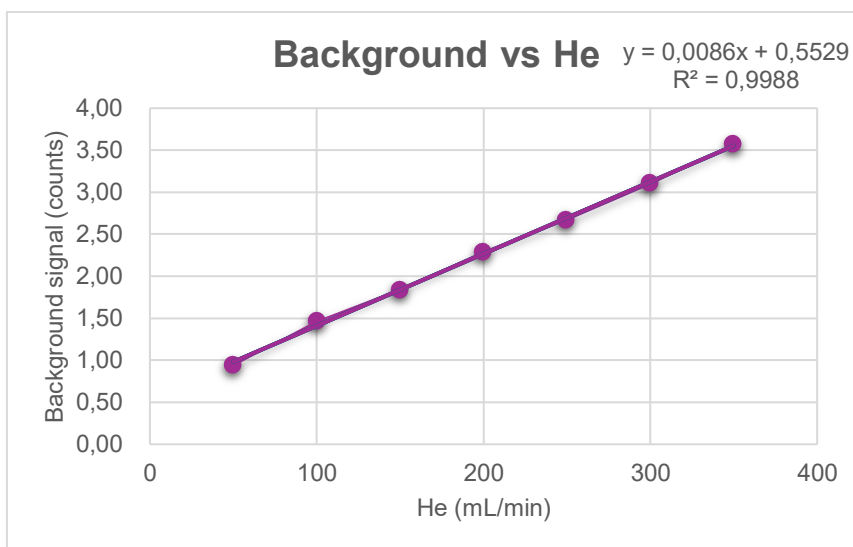


Figure 20. Influence of the He flow rate on the background signal.

### 5.3. Analytical characteristics of MP analysis by LA-SP-ICP-MS

#### 5.3.1. Calibration

The calibration was performed using MP suspensions in water and methanol.

- MPs suspended in water

For this calibration, the following suspensions of PE powder in ultrapure water were prepared: 1, 2, 4, 6, 8 and 10 mg/mL. Measurements from the most concentrated to the least concentrated suspension were performed. However, the results showed that it was very difficult to get a good linearity.

The reason why this linearity cannot be achieved is due to distribution of the MPs in the water drop that changes with the concentration. When depositing the drop, it is easy to observe how the size of the drop changes because of the MPs agglomeration in the center, they are not evenly distributed.

- MPs suspended in methanol

In order to avoid the agglomeration of the MPs in the water drop, the same process was tried using methanol. However, some changes were necessary since the surface tension of methanol is significantly lower than water. When placing the drops in the microscope slide, they would not stay and would spill all over the microscope slide instead. For this reason, the type of microscope slide was changed (Figure 21).



Figure 21. Microscope slide used for PE suspension in methanol.

It was possible to observe that MPs were still agglomerating unevenly as shown in Figure 22. The only difference is that instead of having one big agglomeration of MPs, it was possible to see smaller clusters all over the drop. As a conclusion, methanol did not help to get measurements with good linearity in terms of  $^{13}\text{C}$  peak signals.

Van Acker *et al.*<sup>29</sup> measured the size of different MPs by LA-SP-ICP-MS but they also did not provide information about concentrations.

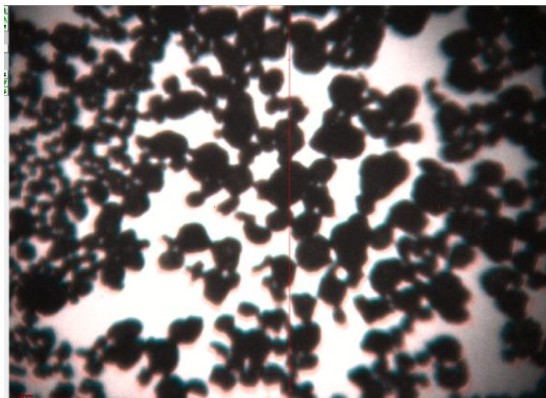


Figure 22. Uneven distribution of the PE MPs in the microscope slide.

### 5.3.2. Reproducibility in the measurements

The reproducibility was studied using MPs deposited on a microscope slide and on a fiberglass filter.

- MPs deposited on a microscope slide

After realizing that the calibration in concentration was not achievable on the microscope slide, a new portion of the 8 mg/mL suspension was introduced as a standard. The conditions were scan speed 20  $\mu\text{m/s}$ , repetition rate 20 Hz, spot size 100  $\mu\text{m}$  and energy 0.5  $\text{J/cm}^2$  (the energy of the laser had been reset by the technical service of ESI NWR). This allows the subsequent measurements to provide more information such as the most frequent size and mean size calculated by the Nano-Syngistix<sup>TM</sup> Software. The most frequent size is the mode; and the mean size is the average between all the MP sizes measured. Another parameter measured is the mean signal intensity of the MP signals. When analysing the sample, peak signals corresponding to MPs are obtained as shown in Figure 23. The  $^{13}\text{C}$  signal intensity is highly linearly correlated with the absolute mass of C.<sup>29</sup>

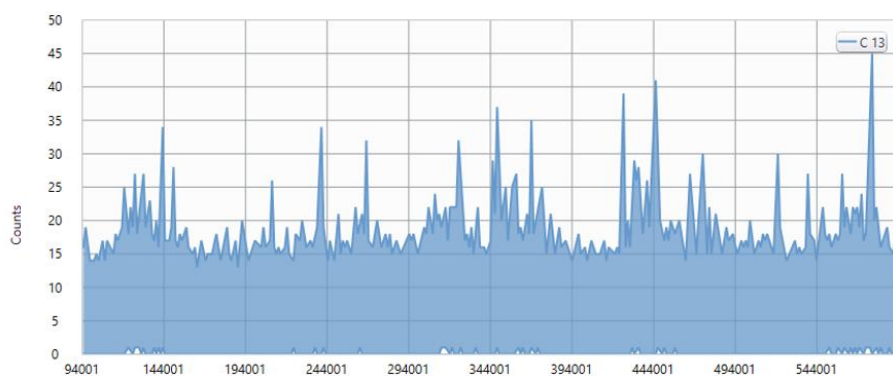


Figure 23. Time scan of a sample containing MPs.

From the time scan, histograms are obtained showing frequency vs. signal intensities or MP size (Figure 24).

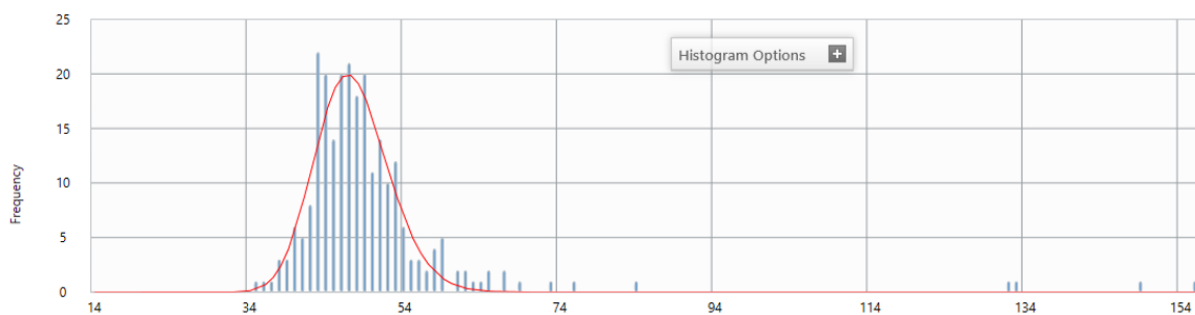


Figure 24. Histogram (frequency vs. size) obtained from the time scan.

Ten measurements of the 8 mg/mL solution were performed, and the results obtained are shown in Table 3.

Table 3. Results obtained for most frequent size, mean size, number of peaks and mean signal intensity when using microscope slides as substrate ( $n = 10$ ).

	Mean	Standard deviation	RSD (%)
Most frequent size	41.8 $\mu\text{m}$	1.7 $\mu\text{m}$	4
Mean size	50.5 $\mu\text{m}$	2.0 $\mu\text{m}$	4
Number of peaks	199.7	45.3	23
Mean signal intensity	66.9 counts	35.1 counts	52

The precision was good in the measurements of size (RSDs < 10 %), but the precision needed for the quantification of the plastics should be improved.

- MPs deposited on a fiberglass filter

Giving that microscope slides have limitations retaining MPs during the measurements when performing the ablation, fiberglass filters with a pore size of 1  $\mu\text{m}$ , shown in Figure 25, were chosen as a more robust substrate.



*Figure 25. Fiberglass filter used instead of microscope slides.*

Figure 26 shows the distribution of the MPs through the fiberglass filter. It is possible to observe that the MPs are still unevenly spread throughout the filter. Leading to the same issue occurred before; the reproducibility in terms of number of  $^{13}\text{C}$  peaks is difficult to achieve.

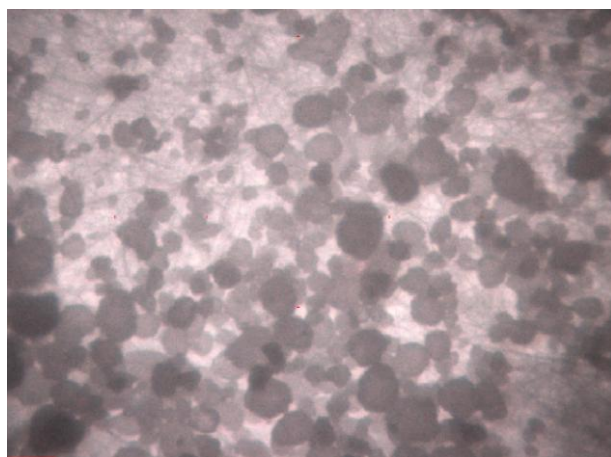


*Figure 26. Polyethylene MPs on the fiberglass filter.*

In terms of the most frequent size, the mean size and the number of peaks, an improvement was observed (lower RSDs). Moreover, the value of the mean intensity is where indeed a significant difference is noticed. The results obtained are shown in Table 4. This improvement shows that, with the fiberglass filter, is easier to introduce a MP at a time, compared to the microscope slide. This could be due to the ability of the fiberglass filter of

retaining the MPs better. The use of these fiberglass filters is ideal for the analysis of filtrated MP samples, e.g. waters.

*Table 4. Results obtained for most frequent size, mean size, number of peaks and mean signal intensity when using fiberglass filters as substrate (n = 8).*

	Mean	Standard deviation	RSD (%)
Most frequent size	47.6 $\mu\text{m}$	1.2 $\mu\text{m}$	3
Mean size	49.8 $\mu\text{m}$	1.6 $\mu\text{m}$	3
Number of peaks	144.3	30.7	21
Mean signal intensity	43.4 counts	4.4 counts	10

### 5.3.3. Limit of detection in size of MPs by LA-SP-ICP-MS

The limit of detection in size (LOD) is derived from the smallest particle that can be detected with reasonable certainty for a given procedure.<sup>33</sup> It is calculated using the value of the background signal and the standard deviation of the background signal.

The LOD calculated by the Nano-Syngistix™ Software was 16  $\mu\text{m}$  after the ablation of a blank on a fiberglass filter, when having a background value of 6 counts. After performing all the measurements, it was observed that getting a background signal lower than 6 counts was very difficult, even when changing carrier gas flow rates or the dwell time.

Hence, the analysis of smaller MPs was performed unsuccessfully. For these experiments, the latex spheres (polystyrene standards) with sizes 2.223, 4.821 and 9.475  $\mu\text{m}$  were employed. Figure 27, Figure 28 and Figure 29 show the pictures of the MPs in the laser ablation chamber.

After, several sets of conditions proposed, all of them resulted in a very small number of signals. These measurements were not consistent. The few peaks obtained had very high intensities and were, probably, due to contaminations. In further investigations, the use of harder and more resistant PEEK tubes to connect the laser ablation chamber with the ICP-MS will be tested in order to reduce the background signal.

Latex MPs were too small to be distinguished from the background signal. In further investigations, the labelling of these smaller MPs with a metal should be also considered in order to achieve their detection.

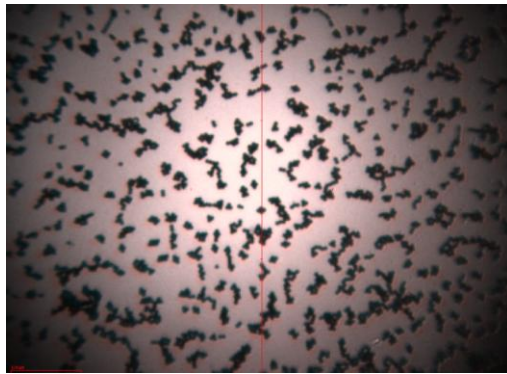


*Figure 27. 9.475  $\mu\text{m}$  latex spheres certified standards in the laser ablation chamber.*

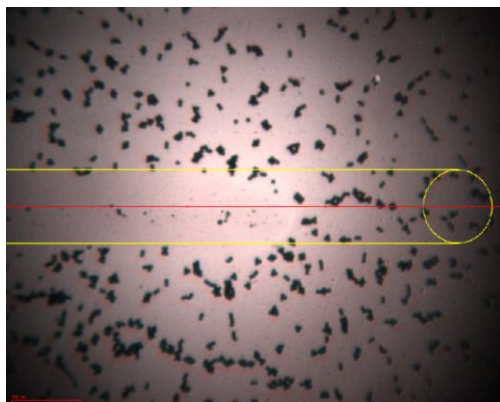


*Figure 28. 4.821  $\mu\text{m}$  latex spheres certified standards in the laser ablation chamber.*

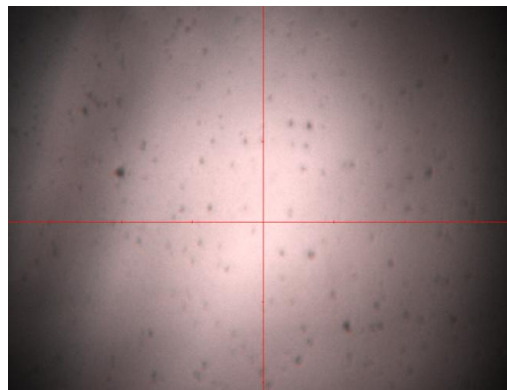


*Figure 29. 2.223  $\mu\text{m}$  latex spheres certified standards in the laser ablation chamber.*

## 6. CONCLUSIONS

### 6.1. Conclusions

The study of the parameters affecting the laser ablation system for MP analysis was successful. Repetition rate and scan speed did not have an influence on the measurements. However, laser ablation energy and spot size were tightly correlated and had a big impact on the results.

The evaluation of important parameters for SP-ICP-MS, such as carrier gas flow rate and dwell time, was performed. The carrier gas flow rate and the dwell have a proportional relationship with the background signal, and a high background signal hinders the detection of smaller MPs.

Calibration in concentration was not possible to achieve due to the changes with MP agglomeration in the drops deposited on glass substrates. Using fiberglass filters, an improvement on the reproducibility was observed due to their ability to retain the MPs.

As a conclusion, the analysis of MPs by LA-SP-ICP-MS is very challenging. In future investigations, the focus should be on developing methods where calibrations in concentration can be achievable. It is also crucial to keep designing methods where MPs smaller than 16  $\mu\text{m}$  can be detected, by reducing the background signal, increasing the sensitivity of the system or labelling these MPs with different metals.

### 6.2. Conclusiones

El estudio de los parámetros que afectan al sistema de ablación láser para el análisis de MP fue exitoso. La frecuencia de disparo del láser y la velocidad de escaneo no influyeron en las medidas. Sin embargo, el diámetro del haz y la energía del láser mostraron una estrecha correlación y tuvieron un gran impacto en los resultados.

Se evaluaron parámetros importantes para SP-ICP-MS, como el caudal del gas portador y el tiempo de permanencia. El caudal del gas portador y el tiempo de permanencia son proporcionales a la señal de fondo, y una señal de fondo alta dificulta la detección de MPs más pequeños.

No fue posible el calibrado en concentración debido a los cambios en la aglomeración de MPs en las gotas depositadas sobre sustratos de vidrio. Utilizando filtros de fibra de vidrio, se observó una mejora en la reproducibilidad gracias a su capacidad para retener los MPs.

En conclusión, el análisis de MPs mediante LA-SP-ICP-MS presenta un gran desafío. En futuras investigaciones, el enfoque debe centrarse en el desarrollo de métodos que permitan conseguir calibrados en concentración. También es importante seguir desarrollando métodos para la determinación de MPs de tamaños menores de 16  $\mu\text{m}$ , ya sea reduciendo la señal de fondo, aumentando la sensibilidad del equipo o etiquetando estos MPs con diferentes metales.

### **6.3. Conclusións**

O estudo dos parámetros que afectan o sistema de ablación láser para a análise de MPs tivo éxito. A taxa de frecuencia de disparo do láser e a velocidade de escaneo non influíron nas medidas. Non obstante, o diámetro e a enerxía do láser estiveron estreitamente correlacionados e tiveron un impacto significativo nos resultados.

Avaliáronse parámetros importantes para SP-ICP-MS, como o caudal do gas portador e o tempo de residencia. O caudal do gas portador e o tempo de residencia son proporcionais ao sinal do fondo, e un sinal de fondo alto dificulta a detección dos MPs máis pequenos.

A calibración en concentración non foi posible debido aos cambios na aglomeración de MPs nas pingas depositadas en substratos de vidro. Usando filtros de fibra de vidro, observouse unha mellora da reproducibilidade debido á súa capacidade para reter MPs.

En conclusión, a análise de MPs mediante LA-SP-ICP-MS presenta un desafío significativo. As futuras investigacións deberíanse centrar no desenvolvemento de métodos que permitan a calibración en concentración. Tamén é importante continuar desenvolvendo métodos para a determinación de MPs de tamaños menores de 16  $\mu\text{m}$ , xa sexa reducindo o sinal de fondo, aumentando a sensibilidade do equipo ou etiquetando estes MPs con diferentes metais.

## 7. REFERENCES

<sup>1</sup> Ziani, K., Ioniță-Mîndrican, C. B., Mititelu, M., Neacșu, S. M., Negrei, C., Moroșan, E., Drăgănescu, D., & Preda, O. T. (2023). Microplastics: A real global threat for environment and food safety: A state of the art review. *Nutrients*, *15*(3), 617. <https://doi.org/10.3390/nu15030617>.

<sup>2</sup> European Commission (2024). Commission's Delegated Decision (EU) 2024/1441 of 11 March 2024 supplementing Directive (EU) 2020/2184 of the European Parliament and of the Council by establishing a methodology to measure microplastics in water intended for human consumption. *Official Journal of the European Union*, document 32024D1441, [https://eur-lex.europa.eu/eli/dec\\_del/2024/1441/oj/eng](https://eur-lex.europa.eu/eli/dec_del/2024/1441/oj/eng).

<sup>3</sup> Plastics Europe. (n.d.). History of plastics. Retrieved April 15, 2025, from <https://plasticseurope.org/plastics-explained/history-of-plastics/>

<sup>4</sup> Science History Institute of Philadelphia. (n.d.). History and future of plastics. Retrieved April 15, 2025, from <https://www.sciencehistory.org/education/classroom-activities/role-playing-games/case-of-plastics/history-and-future-of-plastics/>

<sup>5</sup> Science Museum of London. (2019, October 11). The age of plastic: From Parkesine to pollution. Retrieved April 15, 2025, from <https://www.sciencemuseum.org.uk/objects-and-stories/chemistry/age-plastic-parkesine-pollution>

<sup>6</sup> Chalmin, P. (2019). The history of plastics: from the Capitol to the Tarpeian Rock. Retrieved June 1, 2025, from <https://www.institut.veolia.org/en/history-plastics-capitol-tarpeian-rock>

<sup>7</sup> Naeco Packaging. (2023, May 2). Historia del plástico: origen y evolución. Retrieved April 15, 2025, from <https://naeco.com/es/actualidad/historia-del-plastico/>

<sup>8</sup> United Nations Environment Programme. (2023, April 28). Microplastics: The long legacy left behind by plastic pollution. Retrieved April 15, 2025, from <https://www.unep.org/news-and-stories/story/microplastics-long-legacy-left-behind-plastic-pollution>

<sup>9</sup> European Parliament website. (2018, November 22). Microplásticos: causas, efectos y soluciones. Retrieved April 15, 2025, from <https://www.europarl.europa.eu/topics/es/article/20181116STO19217/microplasticos-causas-efectos-y-soluciones>

<sup>10</sup> Peijnenburg, W. (2025). Airborne microplastics enter plant leaves and end up in our food. *Nature*, 641. <https://doi.org/10.1038/d41586-025-00909-3>

<sup>11</sup> Thacharodi, A., Meenatchi, R., Hassan, S., Hussain, N., Bhat, M. A., Arockiaraj, J., Ngo, H. H., Le, Q. H., & Pugazhendhi, A. (2024). Microplastics in the environment: A critical overview on its fate, toxicity, implications, management, and bioremediation strategies. *Journal of Environmental Management*, 349, 119433. <https://doi.org/10.1016/j.jenvman.2023.119433>

<sup>12</sup> Fundación Aquae. ¿Dónde se encuentran los microplásticos?. Retrieved April 17, 2025, from <https://www.fundacionaquae.org/wiki/dia-mundial-del-medio-ambiente-microplasticos-en-la-tierra-en-el-agua-dulce-y-en-el-mar/>

<sup>13</sup> O'Brien, S., Rauert, C., Ribeiro, F., Okoffo, E. D., Burrows, S. D., O'Brien, J. W., Wang, X., Wright, S. L., Thomas, K. V. (2023). There's something in the air: A review of sources, prevalence and behaviour of microplastics in the atmosphere. *Science of The Total Environment*, 874, 162193. <https://doi.org/10.1016/j.scitotenv.2023.162193>

<sup>14</sup> Torres-Agullo, A., Karanasiou, A., Moreno, T., Lacorte, S. (2021). Overview on the occurrence of microplastics in air and implications from the use of face masks during the COVID-19 pandemic. *National Library of Medicine*, 800, 149555. <https://doi.org/10.1016/j.scitotenv.2021.149555>

<sup>15</sup> Lee, Y., Cho, J., Hassan, S., Sohn, J., Kim, C. (2023). Health effects on microplastic exposure: Current issues and perspectives in South Korea. *Yonsei Medical Journal*, 64 (5), 301-308. <https://doi.org/10.3349/ymj.2023.0048>

<sup>16</sup> National Institute of Environmental Health Sciences. (2023, August). New research highlights the problem of microplastic pollution. Retrieved April 17, 2025, from [https://www.niehs.nih.gov/research/programs/geh/geh\\_newsletter/2023/8/articles/new\\_research\\_highlights\\_the\\_problem\\_of\\_microplastic\\_pollution](https://www.niehs.nih.gov/research/programs/geh/geh_newsletter/2023/8/articles/new_research_highlights_the_problem_of_microplastic_pollution)

<sup>17</sup> Li, Y., Tao, L., Wang, Q., Wang, F., Li, G. Song, M. (2023). Potential health impact of microplastics: A review of environmental distribution, human exposure, and toxic effects. *Environmental & Health*, 1(4), 249-257. <https://doi.org/10.1021/envhealth.3c00052>

<sup>18</sup> Emenike, E. C., Okorie, C. J., Ojeyemi, T., Egbemhenghe, A., Iwuozor, K. O., Saliu, O. D., Okoro, H. K., Adeniyi, A. G. (2023). From oceans to dinner plates: The impact of microplastics on human health. *Heliyon*, 9(10). <https://doi.org/10.1016/j.heliyon.2023.e20440>

<sup>19</sup> Wilschefski, S. C., Baxter, M. R. (2019). Inductively coupled plasma mass spectrometry: Introduction to analytical aspects. *Clinical Biochemist Reviews*, 40(3), 115–133. <https://doi.org/10.33176/AACB-19-00024>

<sup>20</sup> Laborda, F., Bolea, E., & Jiménez-Lamana, J. (2013). Single particle inductively coupled plasma mass spectrometry: A powerful tool for nanoanalysis. *Analytical Chemistry*. 86(5), 2270-2278. <https://doi.org/10.1021/ac402980q>

<sup>21</sup> Mozhayeva, D., Engelhard, C. (2020). A critical review of single particle inductively coupled plasma mass spectrometry – A step towards an ideal method for nanomaterial characterization. *Journal of Analytical Atomic Spectrometry*, 35, 1740-1783. <https://doi.org/10.1039/C9JA00206E>

<sup>22</sup> Brunnbauer, L., Kronlachner, L., Foisner, E., Limbeck, A. (2025). Novel calibration approach for particle size analysis of microplastics by laser ablation single particle-ICP-MS. *Journal of Analytical Atomic Spectrometry*, 40, 753. <https://doi.org/10.1039/d4ja00351a>

<sup>23</sup> Laborda, F., Trujillo, C., Lobinski, R. (2021). Analysis of microplastics in consumer products by single particle inductively coupled plasma mass spectrometry using the carbon-13 isotope. *Talanta*, 221, 121486. <https://doi.org/10.1016/j.talanta.2020.121486>

<sup>24</sup> Sakanupongkul, A., Sirisinha, K., Saenmuangchin, R., Siripinyanond, A. (2024). Analysis of microplastic particles by using single particle inductively coupled plasma mass spectrometry. *Microchemical Journal*, 199, 110016. <https://doi.org/10.1016/j.microc.2024.110016>

<sup>25</sup> Bair, E. C., Guo, Z., Richardson, T. L., Read, J., R. (2024). Quantification of palladium-labelled nanoplastics algal uptake by single cell and single particle inductively coupled plasma mass spectrometry. *Environmental Chemistry*, 21, EN24011. <https://doi.org/10.1071/EN24011>

<sup>26</sup>Kronlachner, L., Gajarska, Z., Becker, P., Günther D., Limbeck, A. (2025). An efficient and stable sample preparation and calibration strategy for nanoparticle analysis using laser ablation single particle-ICP-MS. *Journal of Analytical Atomic Spectrometry*, 40, 467-477. <https://doi.org/10.1039/D4JA00385C>

<sup>27</sup> Metarapi, D., Sala, M., Vogel-Mikus, K., Selih, V. S., Van Elteren, J. T. (2019). Nanoparticle analysis in biomaterials using laser ablation-single particle-inductively coupled plasma mass spectrometry. *Analytical Chemistry*, 91, 6200-6205. <https://doi.org/10.1021/acs.analchem.9b00853>

<sup>28</sup> Shahid, M., Sagadevan, S., Ahmed, W., Zhan, Y., Opaprakasit, P. (2022). Laser ablation. In Sagadevan, S., Podder, J., Mohammad, F. (Ed.), *Metal oxides for optoelectronics and optics-based medical applications* (pp. 3-31). Elsevier. <https://doi.org/10.1016/C2020-0-01693-2>

<sup>29</sup> Van Acker, T., Rua-Ibarz, A., Vanhaecke, F., Bolea-Fernandez, E. (2023). Laser ablation for nondestructive sampling of microplastics in single-particle ICP-mass spectrometry. *Analytical Chemistry*, 95, 18579-18586. <https://doi.org/10.1021/acs.analchem.3c04473>

<sup>30</sup> Wang, M., Zheng, L., Wang, B., Yang, P., Fang, H., Liang, S., Chen, W., Feng, W. (2022). Laser ablation-single particle-inductively coupled plasma mass spectrometry as a sensitive tool for bioimaging of silver nanoparticles *in vivo* degradation. *Chinese Chemical Letters*, 33, 3484-3487. <https://doi.org/10.1016/j.ccllet.2022.03.098>

<sup>31</sup> Diwakar, P. K., Gonzalez, J. J., Harilal, S. S., Russo, R. E., Hassanein, A. (2013). Ultrafast laser ablation ICP-MS: role of spot size, laser fluence, and repetition rate in signal intensity and elemental fractionation. *Journal of Analytical Atomic Spectrometry*, 29, 339. <https://doi.org/10.1039/c3ja50315a>

<sup>32</sup> Lee, J. S., Lee, D. S., Park, C. J., Jeon, M. S., Lee, H. S. (2009). The influence of carrier gas in the analysis of alumina by laser ablation inductively coupled plasma mass spectrometry. *Current Applied Physics*, 9, S280-S283. <https://doi.org/10.1016/j.cap.2009.01.038>

<sup>33</sup> PerkinElmer. (2019). Syngistix™ Software for ICP-MS v.2.5. Software reference guide. PerkinElmer.